Universiteit Leiden
The Netherlands

The non-coordinating anion 1,1,3,3-tetracyano-2-propoxy-propenide as an anion-pi donor in cis-diaquabis(2,2 '-dipyridylamine)zinc and its cadmium analog: Luminescence properties, Hirshfeld analysis and central-atom induced polymorphism

Lehchili, F.; Setifi, F.; Liu, X.; Saneei, A.; Kucerakova, M.; Setifi, Z.; ... ; Reedijk, J.

Citation
Lehchili, F., Setifi, F., Liu, X., Saneei, A., Kucerakova, M., Setifi, Z., ... Reedijk, J. (2017). The non-coordinating anion 1,1,3,3-tetracyano-2-propoxy-propenide as an anion-pi donor in cis-diaquabis(2,2 '-dipyridylamine)zinc and its cadmium analog: Luminescence properties, Hirshfeld analysis and central-atom induced polymorphism. *Polyhedron*, *131*, 27-33. doi:10.1016/j.poly.2017.04.020

Version: Not Applicable (or Unknown)
License: Leiden University Non-exclusive license
Downloaded from: https://hdl.handle.net/1887/57556

Note: To cite this publication please use the final published version (if applicable).

Polyhedron 131 (2017) 27–33

Contents lists available at ScienceDirect

Polyhedron

journal homepage: www.elsevier.com/locate/poly

The non-coordinating anion 1,1,3,3-tetracyano-2-propoxy-propenide as an anion-π donor in cis-diaquabis(2,2′-dipyridylamine)zinc and its cadmium analog: Luminescence properties, Hirshfeld analysis and central-atom induced polymorphism

Fouzia Lehchili [a], Fatima Setifi [a,b,*], Xue Liu [c], Anahid Saneei [d], Monika Kučeráková [e], Zouaoui Setifi [b], Michal Dušek [e], Morgane Poupon [e], Mehrdad Pourayoubi [d,*], Jan Reedijk [c,*]

[a] Unité de Recherche de Chimie de l'Environnement et Moléculaire Structurale (CHEMS), Université Constantine 1, Constantine 25000, Algeria
[b] Laboratoire de Chimie, Ingénierie Moléculaire et Nanostructures (LCIMN), Université Ferhat Abbas Sétif 1, Sétif 19000, Algeria
[c] Leiden Institute of Chemistry, Leiden University, P.O. Box 9502, 2300 RA Leiden, The Netherlands
[d] Department of Chemistry, Faculty of Sciences, Ferdowsi University of Mashhad, Mashhad, Iran
[e] Institute of Physics ASCR, Na Slovance 2, 182 21 Prague, Czech Republic

ARTICLE INFO

Article history:
Received 19 February 2017
Accepted 18 April 2017
Available online 26 April 2017

Keywords:
Polynitrile
Crystal structure
Anion-π interaction
Luminescence
Hirshfeld surface

ABSTRACT

The synthesis, structure and properties of cis-diaquabis(2,2′-dipyridylamine)zinc bis(1,1,3,3-tetracyano-2-propoxy-propenide), $[Zn(H_2O)_2(2,2'\text{-dpa})_2][tcnopr]_2$, **I**, and its isomorphous Cd analog, **II**, are reported. These two coordination compounds were prepared through hydrothermal reactions of Zn(II)/Cd(II) acetate with potassium 1,1,3,3-tetracyano-2-propoxy-propenide ($tcnopr^- = [(NC)_2CC(OPr)C(CN)_2]^-$) in the presence of 2,2′-dipyridylamine (dpa = $C_{10}H_9N_3$) as a co-ligand. Both new compounds were fully characterized by elemental analysis, FT-IR spectroscopy, powder XRD and X-ray single-crystal diffraction.

Single-crystal X-ray analysis has revealed that compounds **I** and **II** are isostructural containing octahedrally coordinated metal ions, and exhibit 3D supramolecular architectures, including multiple anion-π interactions. Furthermore, the photoluminescence properties in the solid state at room temperature and Hirshfeld surfaces analysis to understand the packing have also been investigated in detail.
© 2017 The Authors. Published by Elsevier Ltd. This is an open access article under the CC BY-NC-ND license (http://creativecommons.org/licenses/by-nc-nd/4.0/).

1. Introduction

Luminescent materials based on transition metals and lanthanoids have found wide applications in lighting [1–4], luminescence sensing [5–7] and optical devices [8]. Among them, d^{10} metal coordination compounds comprising zinc(II) and cadmium (II) with a variety of ligands, have drawn extensive attention in the past decades due to their attractive luminescence properties [3,9–11].

In the last decade the phenomenon of supramolecular interactions involving electron poor π systems and lone pairs or anions has become a topic of both fundamental and practical interest [12–18], e.g. for isolation and binding of anions. Ligands like aminopyridines and other heteroaromatic rings have shown to be good acceptors for such anion binding [18,19].

Organic polynitrile ligands are versatile structural components, leading to many different architectures in zero, one, two or three dimensions, and incorporating most of the 3d transition metals [20–25]. The versatility of such ligands is based on two main properties i.e.: (i) the ability to act as often rigid ligand bridges, given the linear and rigid geometry of the CN groups, and (ii) the possibility of functionalization with different potentially coordinating groups that leads to a high variety of coordination modes. The occurrence of non-coordinating polynitriles appears to be rare and unprecedented.

To explore this coordination and packing behavior in more details, we have been using one of these polynitrile organic anions in combination with other chelating or bridging neutral co-ligands for the study of the structural and electronic characteristics of the resulting coordination compounds. In particular, attention was given to molecular materials exhibiting interesting luminescence behavior, like d^{10} ions zinc and cadmium.

As a matter of fact feeble anion-π interactions are often a controlling factor to direct the self-assembly of metal complexes

* Corresponding authors. at: Leiden Institute of Chemistry, Leiden University, P.O. Box 9502, 2300 RA Leiden, The Netherlands. Fax: +31 715274671 (J. Reedijk).
E-mail addresses: fat_setifi@yahoo.fr (F. Setifi), pourayoubi@ferdowsi.um.ac.ir (M. Pourayoubi), Reedijk@chem.leidenuniv.nl (J. Reedijk).

http://dx.doi.org/10.1016/j.poly.2017.04.020
0277-5387/© 2017 The Authors. Published by Elsevier Ltd.
This is an open access article under the CC BY-NC-ND license (http://creativecommons.org/licenses/by-nc-nd/4.0/).

generating supramolecular networks [26,27]. Very recently, crystallographic evidence was reported for $ClO_4^- \cdots \pi$ interactions, acting as a supramolecular glue to connect 2-D layers, formed by a Cu(II) coordination entity cation, into a 3-D network [28].

In this work, we report on the synthesis of the first luminescent series of mononuclear zinc(II) and cadmium(II) coordination compounds containing the organic polynitrile 1,1,3,3-tetracyano-2-propoxy-propenide counter anion (abbreviated as tcnopr$^-$) in combination with the chelating ligand 2,2′-dipyridylamine (abbreviated as dpa). The characterization and structure determinations of the compounds were performed through infrared spectroscopy, elemental analysis, X-ray crystallography and powder X-ray diffraction. The photophysical properties were studied by solid-state absorption spectra and further by solid-state excitation and emission spectra.

Hirshfeld surface analysis was used for the study of the intermolecular packing interactions and visualization of moderate and week hydrogen bonds and anion-π stacking.

2. Experimental

2.1. Reagents and techniques

Tetracyanoethene, urea, potassium t-butoxide (C_4H_9OK), malononitrile ($CH_2(CN)_2$), 2,2′-dipyridylamine, $Cd(CH_3COO)_2{\cdot}2H_2O$ and $Zn(CH_3COO)_2{\cdot}2H_2O$ were purchased from Sigma–Aldrich and used without further purification. Solvents were used and purified by standard procedures. Elemental analyses (C, H and N) were performed using a Perkin-Elmer 2400 series II CHN analyzer. Infrared spectra were recorded in the range 4000–50 cm^{-1} on a FT-IR Bruker ATR Vertex 70 Spectrometer. Solution NMR spectra were recorded on a Bruker Avance 300 MHz in D_2O. The excitation and emission spectra were recorded at room temperature using a Shimadzu RF-5301PC spectrofluoriphotometer equipped with a Shimadzu solid-state sample holder.

2.2. X-ray crystallography

Suitable single crystals of **I** and **II** were chosen for an X-ray diffraction study. Crystallographic measurements were done at 120 K with a four-circle CCD diffractometer, Gemini of Oxford Diffraction, using Mo Kα radiation from a classical sealed tube monochromated by graphite and collimated by fiber-optics Enhance collimator. As a detector, we used the CCD detector Atlas S2. Crystal structures were easily solved by charge flipping with program SUPERFLIP [29] and refined with the Jana2006 program package [30] by full-matrix least-squares technique on F^2. The molecular structure plots were prepared by Diamond software [31]. All hydrogen atoms were discernible in difference Fourier maps and could be refined to reasonable geometry. According to common practice, H atoms bonded to C were kept in ideal positions with C–H = 0.96 Å while H atoms bonded to N were refined with N–H distance restraint defining equality of such bonds in the structure model. For all hydrogen atoms we kept U_{iso}(H) equal to 1.2 U_{eq}(C/N). All non-hydrogen atoms were refined using harmonic refinement. Crystallographic data and details of the data collection and structure solution and refinements are listed in Table 1.

Powder samples were measured with an Empyrean diffractometer of PANalytical with Cu Kα radiation and a Nickel beta filter in the 2θ range of 10–80°. Profile parameters were refined with Jana2006 [30].

2.3. Synthesis

The potassium salt of 1,1,3,3-tetracyano-2-propoxy-propenide, K(tcnopr) was synthesized based on recipe for a related compound [32]. Tetracyanoethene (3.2 g, 25 mmol) and urea (1.5 g, 25 mmol) were dissolved in 40 mL of propan-1-ol and warmed to 25 °C during 4 h. Solvent was removed under vacuum and the solid was extracted with 20 mL of a 1:1 water/diethyl ether mixture. The aqueous phase was extracted two more times with 20 mL of diethyl ether. The organic fraction was dried ($MgSO_4$) and the solvent removed to give the 1,1-dicyano-2,2-dipropanoethene as a yellow oil. (3.28 g; 67%). IR data (ν/cm^{-1}): 2973(s), 2928(m), 2882(m), 2229(w), 2216(w), 2206(w), 2174(w), 1747(w), 1729(w), 1642(w), 1551(m), 1380(m), 1324(s), 1271(w), 1174(w), 1087(s), 1045(s), 880(s), 825(m), 801(w), 430(m).

The yellow oil of 1,1-dicyano-2,2-dipropanoethene (2.90 g, 15 mmol) was dissolved in 40 mL of EtOH and a mixture of $CH_2(CN)_2$ (1.00 g, 15 mmol) and tBuOK (1.67 g, 15 mmol) in EtOH

Table 1
Crystal data and structure refinement parameters for compounds **I** and **II**.

	Compound **I**	Compound **II**
Empirical formula	$C_{40}H_{36}N_{14}O_4Zn$	$C_{40}H_{36}N_{14}O_4Cd$
Formula weight	842.2	889.2
T (K)	120.00(10)	120.00(10)
λ (Å)	0.71073	0.71073
Crystal system	monoclinic	monoclinic
Space group	*C*2/*c*	*C*2/*c*
Unit cell dimensions		
a (Å)	19.6133(7)	28.1744(6)
b (Å)	7.5535(2)	7.8571(2)
c (Å)	28.1427(9)	18.9679(5)
β (°)	105.862(3)	104.493(2)
V (Å^3)	4010.6(2)	4065.29(18)
Z	4	4
D_{calc} (g/cm^3)	1.3948	1.4529
Absorption coefficient (mm^{-1})	0.673	0.597
F(000)	1744	1816
Index ranges	$-26 \le h \le 25$, $-10 \le k \le 9$, $-38 \le l \le 38$	$-35 \le h \le 38$, $-10 \le k \le 10$, $-23 \le l \le 25$
Reflections collected	32233	33357
Independent reflections (R_{int})	5255 [0.046]	5302 [0.046]
Refinement method	Full-matrix least-squares on F^2	Full-matrix least-squares on F^2
Data/restraints/parameters	5255/0/276	5302/6/295
Goodness-of-fit (GoF) on F^2	1.40	1.19
Final R indices [$I > 3\sigma(I)$]	R_1 = 0.0330, wR_2 = 0.0879	R_1 = 0.0298, wR_2 = 0.0362
R indices (all data)	R_1 = 0.0448, wR_2 = 0.0932	R_1 = 0.0421, wR_2 = 0.0395
Largest difference peak and hole (e Å^{-3})	0.36 and −0.36	0.34 and −0.44

(40 mL) was poured on it. The resultant solution was stirred under reflux for 2 h, and allowed to cool before being placed in a freezer to obtain K(tcnopr) as an orange powder. (2.45 g, 69%). IR data (ν/cm^{-1}): 2973(w), 2942(w), 2929(w), 2881(w), 2224(w), 2201(s), 2152(m), 1482(s), 1430(s), 1382(m), 1364(s), 1348(s), 1275(w), 1252(w), 1225(w), 1178(s), 1144(w), 1046(m), 930(s), 896(m), 860(m), 707(m), 623(w), 571(w), 540(s), 477(m). NMR ^{1}H (300 MHz, D_2O): 1.00 (t, 3H, J = 7.4 Hz, CH_3); 1.77 (m, 2H, CH_2); 4.35 (t, 2H, J = 6.4 Hz, CH_2O). NMR ^{13}C (125 MHz, D_2O): 12.37 (–**C**H$_3$), 25.64 (–**C**H$_2$–CH$_3$), 48.75 (–**C**(CN)$_2$), 80.80 (–**C**H$_2$–O–), 121.17 (–**C**N), 186.62 (–O–**C**(C(CN)$_2$)$_2$). *Anal. Calc.* for $KC_{10}H_7N_4O$: C, 50.41; N, 23.51; H, 2.96. Found: C, 50.13; N, 23.76; H, 2.82 (%).

Compound **(I)** was synthesized hydrothermally under autogenous pressure from a mixture of $Zn(OAc)_2{\cdot}2H_2O$ (0.2 mmol, 45 mg), dpa (0.1 mmol, 20 mg) and Ktcnopr (0.4 mmol, 80 mg) in water–methanol (4:1 v/v, 20 mL). This mixture was sealed in a Teflon-lined autoclave and heated at 150 °C for 2 days. After cooling to room temperature at a rate of 10 °C h^{-1}, colorless crystals were obtained containing **I**, and some impurities that could be manually separated. A powder profile of the Zn compound is shown in Fig. S1. Elemental analysis and IR data for hand-picked crystals: *Anal. Calc.* for $C_{40}H_{36}ZnN_{14}O_4$ (842.2 g/mol): C, 57.04; H, 4.31; N, 23.28. Found: C, 57.45; H, 4.26; N, 23.69 (%). Main IR data (ν/cm^{-1}): ν(N–H) 3419(br); ν(C≡N) 2196(s); ν(C=N) 1594(m).

Compound **(II)** was synthesized under similar conditions to that of complex (**I**), except that $Cd(OAc)_2{\cdot}2H_2O$ (0.2 mmol, 55 mg) was used instead of $Zn(OAc)_2{\cdot}2H_2O$. Yellow colored crystals were obtained containing **II**, and some impurities that could be manually separated. The powder profile of the Cd compound (**II**) is shown in Fig. S2. Elemental analysis and IR data for hand-picked crystals: *Anal. Calc.* for $C_{40}H_{36}CdN_{14}O_4$ (889.2 g/mol): C, 54.03; H, 4.08; N, 22.05. Found: C, 54.52; H, 3.98; N, 22.18 (%). Main IR data (ν/cm^{-1}): ν(N–H) 3443(br); ν(C≡N) 2193(s); ν(C=N) 1629(m).

3. Results and discussion

3.1. Synthesis and characterization

The starting salt K(tcnopr) was characterized by IR and NMR (^{1}H and ^{13}C in D_2O), and further used in the synthesis of the two new compounds. The elemental analysis and infrared spectra of the compounds **I** and **II** were performed on a pure phase, manually separated under a binocular microscope. The impurities in the bulk samples, mentioned above, are ascribed to products that result from partial decomposition of the polynitrile anions under the hydrothermal conditions. Repeated syntheses using varied temperatures and time exposition on the hydrothermal synthesis did not change or remove these impurities. Both compounds were obtained in good yields and in monocrystalline form, with the expected elemental analyses (*vide supra*). The IR spectra of manually separated crystals of both **I** and **II** display a strong absorption band at 2196 cm^{-1} and 2193 cm^{-1}, respectively, assignable to the $\nu_{(CN)}$ vibration of the tcnopr anionic unit. Compared to the corresponding potassium salt K(tcnopr) containing the non-coordinated tcnopr moiety ($\nu_{(CN)}$: 2201 cm^{-1}), this value is indicative of the presence of non-coordinated tcnopr units in both complexes, as shown by the crystal structure analysis (*vide infra*).

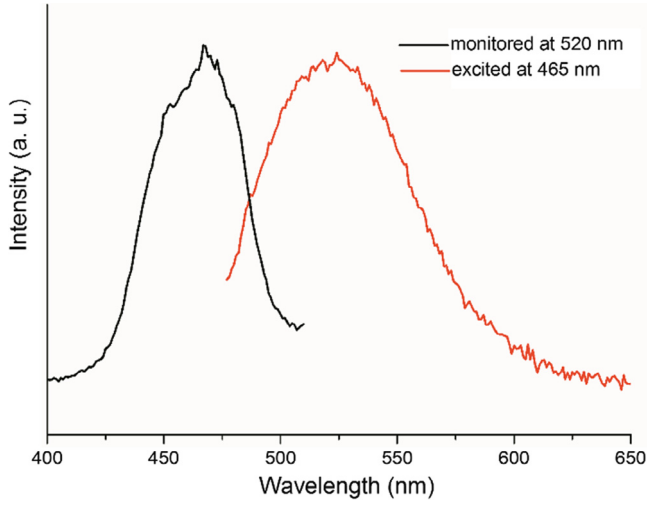

Fig. 1a. Room temperature solid-state excitation (black) and emission (red) spectra of compound **I**. Intensities are in arbitrary units (a.u.). (Color online.)

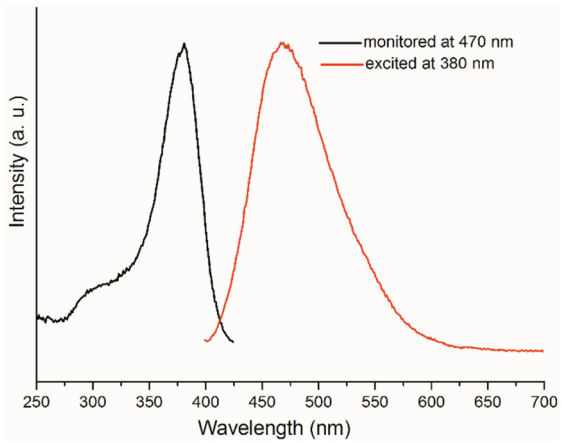

Fig. 1b. Room temperature solid state excitation (black) and emission (red) spectra of compound **II**. Intensities are in arbitrary units (a.u.). (Color online.)

3.2. Emission and excitation spectra

Room temperature solid-state emission and excitation spectra of compounds **I** and **II** have been recorded on pure crystalline phases and are shown in Figs. 1a and 1b. When excited at 465 nm light, compound **I** shows a relatively weak emission. Only one broad band was observed in the emission spectrum with a maximum at about 520 nm, which can be ascribed to the ligand π–π^* transition based on literature studies [33–37]. The excitation spectrum of compound **I** contains a broad band with a maximum at 465 nm.

Under irradiation at 380 nm UV light, compound **II** exhibits a medium intense emission. The emission spectrum of compound **II** consists of only one broad peak from 450 nm to 650 nm with a maximum at around 470 nm, which also can be assigned to ligand π–π^* transition [33–37]. The excitation spectrum of the Cd compound, **II**, shows a broad band with a maximum at 380 nm.

3.3. Description of the crystal structures

Structures of the compounds **I** and **II** were calculated using the same monoclinic $C2/c$ space group, see Table 1 (above). However, the parameters a and c must be swapped for such a description. In order to keep the same order of the very similar unit cell parameters, one of the structures would get symmetry $A2/a$. This is just a manifestation of different packing of otherwise very similar compounds.

The asymmetric unit of both compounds contains one half of the cation $[M(H_2O)_2(2,2'\text{-dpa})_2]^{2+}$ M = Zn (**I**), Cd (**II**), and one non-coordinated anion (tcnopr)$^-$. The metal is located at the special

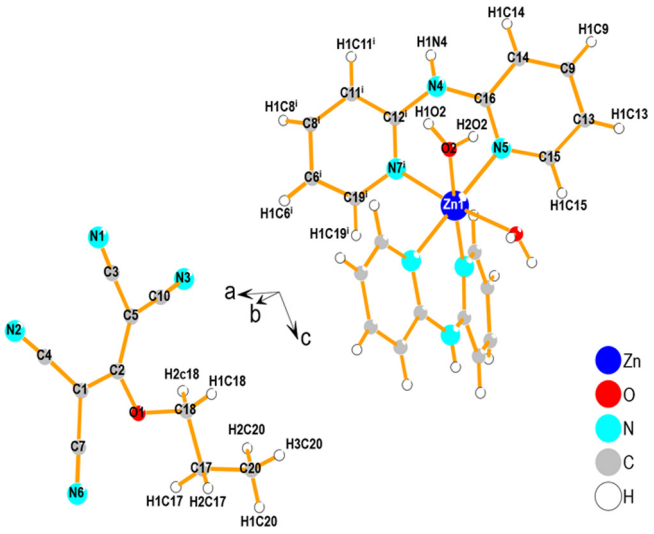

Fig. 2a. Molecular cationic and anionic species of $[Zn(H_2O)_2(2,2'\text{-dpa})_2][tcnopr]_2$, with the atom labels displayed. Symmetry code (i) $-x + 1, y, -z + 1/2$.

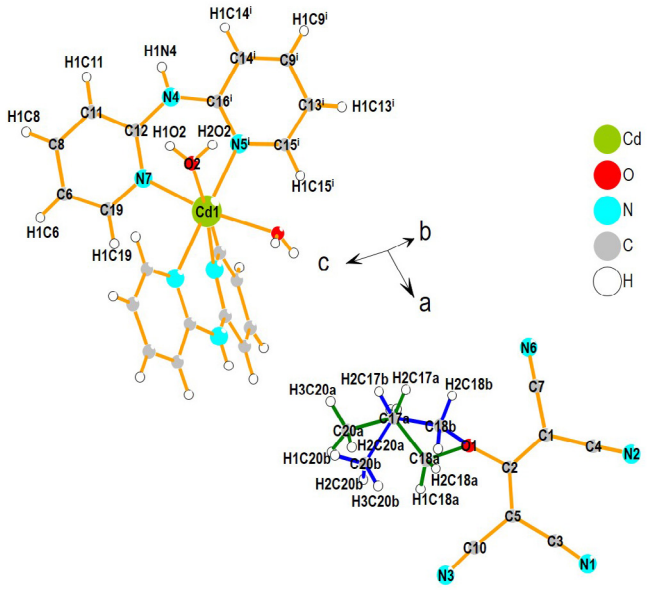

Fig. 2b. Molecular cationic and anionic species of $[Cd(H_2O)_2(2,2'\text{-dpa})_2][tcnopr]_2$, with the atom labels displayed. Symmetry code (i) $-x + 1, y, -z + 1/2$. Disordered parts of the $CH_3CH_2CH_2$ chain are distinguished by green (part **a**) and blue (part **b**) bonds. (Color online.)

position 4e. Molecular species of both compounds are depicted in Figs. 2a and 2b.

For the Cd compound, the $C20H_3$-$C17H_2$-$C18H_2$ branch of the $(tcnopr)^-$ anion is disordered over two positions (lower part of figure), which are occupied 0.7921(9) for the chain **a** and 0.2078(1) for the chain **b**. The M(II) ions have an octahedral cis-MO_2N_4 environment with the cis nitrogen donor atoms belonging to a chelating 2,2′-dpa ligand.

The metal centers are located on a C2 rotation axis, bisecting the O–M–O^i angles in which oxygen atoms come from the aqua ligands. The distances M–N (Zn1–N5 = 2.1440(11) Å, Zn1–N7 = 2.1123(13) Å, Cd1–N5 = 2.3146(14) Å and Cd1–N7 = 2.3060 (16) Å) and M–O (Zn1–O2 = 2.1375(11) Å and Cd1–O2 = 2.3075 (15) Å) are in the normal ranges and consistent with those observed in analogous structures [20,38]. Summary of relevant bond lengths and angles is given in Table 2.

Table 2
Relevant bond lengths (Å) and angles (°) for structures **I** and **II**, symmetry code: (i) $-x + 1, y, -z + 1/2$.

I		**II**	
Zn1–O2	2.1375(11)	Cd1–O2	2.3075(15)
Zn1–$O2^i$	2.1375(11)	Cd1–$O2^i$	2.3075(15)
Zn1–N5	2.1440(11)	Cd1–N5	2.3146(14)
Zn1–$N5^i$	2.1440(11)	Cd1–$N5^i$	2.3146(14)
Zn1–N7	2.1123(13)	Cd1–N7	2.3060(16)
Zn1–$N7^i$	2.1123(13)	Cd1–$N7^i$	2.3060(16)
O1–C2	1.348(2)	O1–C2	1.344(3)
O1–C18	1.441(2)	O1–C18a	1.425(3)
N1–C3	1.141(2)	N1–C3	1.146(3)
N2–C4	1.144(2)	N2–C4	1.150(3)
N3–C10	1.152(2)	N3–C10	1.147(3)
N4–$C12^i$	1.3872(18)	N4–C12	1.383(2)
N4–C16	1.384(2)	N4–$C16^i$	1.392(3)
N5–C15	1.357(2)	N5–C15	1.359(3)
N5–C16	1.341(2)	N5–C16	1.337(2)
N6–C7	1.149(2)	N6–C7	1.145(3)
N7–C12	1.3376(17)	N7–C12	1.333(2)
N7–C19	1.3561(18)	N7–C19	1.348(2)
O2–Zn1–$O2^i$	83.272(1)	O2–Cd1–$O2^i$	92.30(5)
O2–Zn1–N5	86.07(4)	O2–Cd1–N5	89.30(5)
O2–Zn1–$N5^i$	90.71(4)	O2–Cd1–$N5^i$	90.20(5)
O2–Zn1–N7	173.86(4)	O2–Cd1–N7	169.73(5)
O2–Zn1–$N7^i$	91.20(4)	O2–Cd1–$N7^i$	88.92(6)
$O2^i$–Zn1–N5	90.706(1)	$O2^i$–Cd1–N5	90.20(5)
$O2^i$–Zn1–$N5^i$	86.07(4)	$O2^i$–Cd1–$N5^i$	89.30(5)
$O2^i$–Zn1–N7	91.203(1)	$O2^i$–Cd1–N7	88.92(6)
$O2^i$–Zn1–$N7^i$	173.86(4)	$O2^i$–Cd1–$N7^i$	169.73(5)
N5–Zn1–$N5^i$	175.70(5)	N5–Cd1–$N5^i$	179.28(6)
N5–Zn1–N7	96.72(5)	N5–Cd1–N7	100.89(5)
N5–Zn1–$N7^i$	86.21(5)	N5–Cd1–$N7^i$	79.62(5)
$N5^i$–Zn1–N7	86.21(5)	$N5^i$–Cd1–N7	79.62(5)
$N5^i$–Zn1–$N7^i$	96.72(5)	$N5^i$–Cd1–$N7^i$	100.89(5)
N7–Zn1–$N7^i$	94.46(5)	N7–Cd1–$N7^i$	91.70(6)

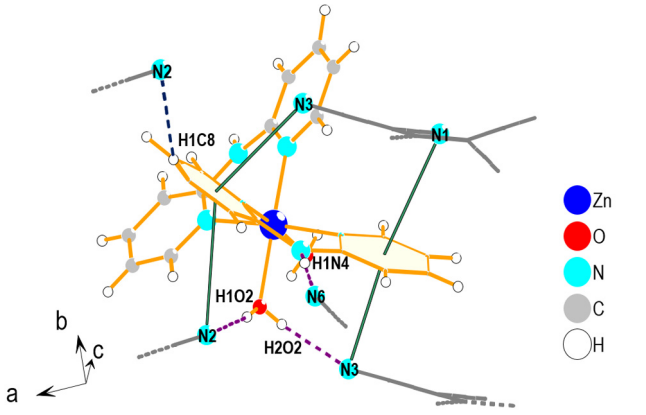

Fig. 3. Molecular packing of the compound **I**. Color codes: full orange lines = Zn-complex cation; full lines in gray = $(tcnopr)^-$ anion; dashed purple lines = moderately strong hydrogen bonds; dashed dark blue lines = weak hydrogen bonds; full green lines = anion···π-stacking. (Color online.)

Figs. 3 and 4 show non-bonding interactions in the compounds **I** and **II**, using the color codes (see the figure caption) distinguishing moderate hydrogen bonds, weak hydrogen bonds and anion···π-stacking. In both structures, three moderately strong hydrogen bonds can be noticed between the NH unit of the 2,2′-dipyridylamine ligand, the aqua ligand and nitrogen atoms of $(tcnopr)^-$ anion (Table S1). Here, typical hydrogen bonded N···N contacts are 2.98–3.00 Å and O···N contacts are 2.81–2.95 Å.

For the compound **I**, the $(tcnopr)^-$ anion is connected only with the Zn-complex while in the compound **II** there is a weak hydrogen interaction between two $(tcnopr)^-$ anions. This weak interaction

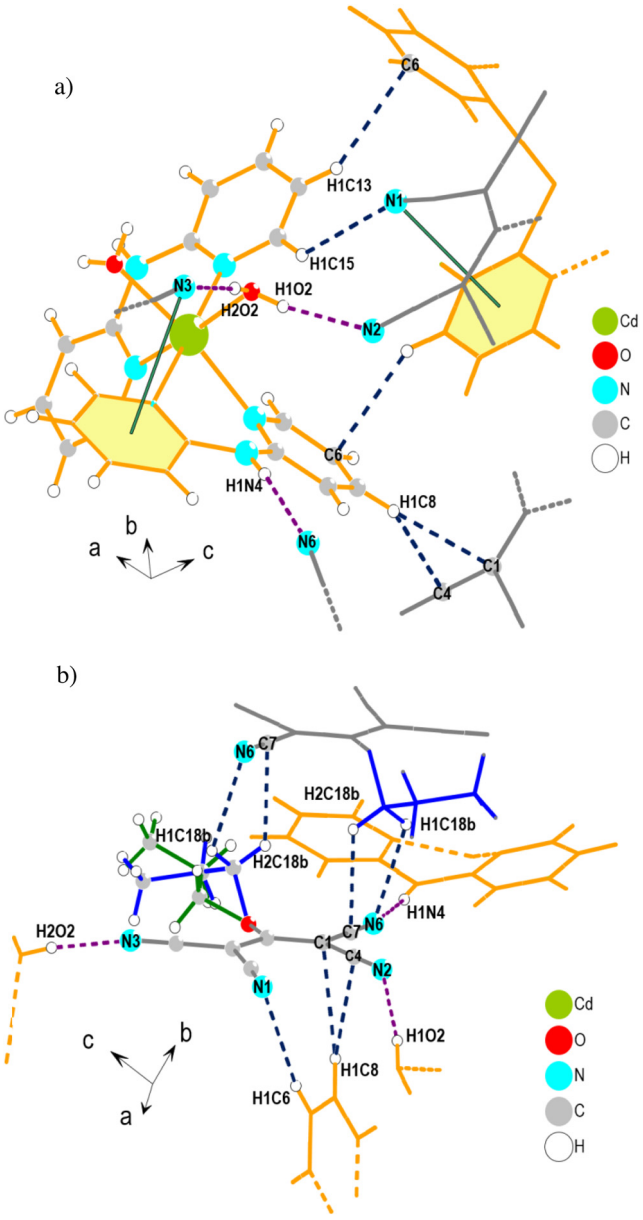

Fig. 4. Two views of molecular packing of compound **II**. Top figure: bounding around the Cd cationic species, Bottom figure: bounding around $(tcnopr)^-$ anion. Color codes: full orange lines = Cd cationic species; full lines in gray = $(tcnopr)^-$ anion; dashed purple lines = moderately strong hydrogen bonds; dashed dark blue lines = weak hydrogen bonds; full green lines = anion…π-stacking. Disordered parts of the $(tcnopr)^-$ anion in the bottom figure are distinguished by full blue and green lines. (Color online.)

seems to be responsible for disorder of $CH_3CH_2CH_2$ group. Indeed, only the chain **b** (blue in Fig. 4b) interacts with the nitrile part of the second $(tcnopr)^-$ anion (Fig. 4b). Hydrogen atoms H1C18b and H2C18b have the respective distances to N6 of 2.5095(30) Å and C7 of 2.4232(23) Å.

The anion-π stacking interactions are observed between pyridyl rings of 2,2′-dpa ligand and nitrile groups of $(tcnopr)^-$ anion. For both compounds **I** and **II** this interaction appears for both rings, namely for the rings C15–C13–C9–C14–C16–N5 (R1) and C19–C6–C8–C11–C12–N7 (R2). So, in compound **I**, R1 and R2 are connected to the nitrile group nitrogen atoms with separations of 3.3987(1) Å for N1···R1, 3.3179(1) Å for N3···R1, 3.6469(1) Å for N2···R2 and 3.2920(1) Å for N3···R2. In compound **II**, R1 ring involved in two anion···π stacking, N1···R1 3.5478(22) Å and N3···R1 3.5136(23) Å, while R2 is involved in only one anion···π interaction, N3···R2 = 3.2975(2) Å and due to the distance between R2 and N2 is too long (3.9974(1) Å), it can hardly be considered as an effective interaction. So the differences in packing between both compounds are probably related to these weaker interactions.

All these interactions may be regarded as very weak, according to the sum of the van der Waals radii of C and N atoms (3.25 Å) [39]. Among these interactions, the shortest N3···π(R2) distance in **I** and **II** corresponds to the angle of 82.67° and 83.13°. The other angles subtended by the N2···π, N1···π and N3···π axes to the planes of the aromatic rings are as follow: 58.54° (N2···R2 in **I**), 70.60° (N1···R1 in **I**), 82.71° (N3···R1 in **I**), 71.623° (N1···R1 in **II**), 76.45° (N3···R1 in **II**). More details of this type of interaction could be visualized using a Hirshfeld analysis (see below).

3.4. Hirshfeld surface analysis

For a better understanding of the packing in the crystal with a variety of interactions, we used the Hirshfeld surface (HS) analysis, which uses three-dimensional (3D) surface functions, and two-dimensional (2D) fingerprint plots [40–42]. This method is very convenient to visualize intermolecular interactions and highlight the similarity and differences in different packing maps.

The Hirshfeld surfaces (HSs) mapped with d_{norm} and corresponding shape index associated 2D fingerprint plots (FPs) of compounds **I** and **II** were generated using the *CrystalExplorer* software version 3.1 [43] and structures of **I** and **II** entered in the CIF format. Fig. 5 shows results for cations abbreviated $Zn[O]_2[N_2]_2$ and $Cd[O]_2[N_2]_2$, and Fig. 6 presents similar information for the anions.

The two isostructural compounds have HS maps with minor difference related to the slight differences in the crystal packing. On the HSs of cationic components in both structures two large red areas can be noticed (labels 1 and 2 in Fig. 5a and b), which correspond to two O–H···N hydrogen bonds formed between aqua oxy-

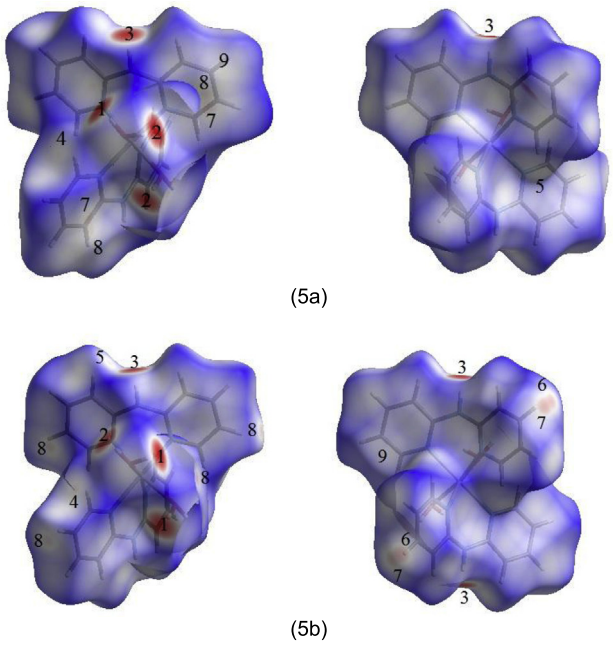

Fig. 5. Views of the Hirshfeld surfaces in two orientations for the $M[O]_2[N_2]_2$ cation of **I** & **II**: (a) $Zn[O]_2[N_2]_2$ cation, (b) $Cd[O]_2[N_2]_2$ cation, (HSs are mapped with d_{norm}). Labels on HSs are as follows: O2–H1*o*2···N2 (**1**), O2–H2*o*2···N3 (**2**), N4–H1*n*4···N6 (**3**), C15–H1*c*15···N1 (**4**), C19–H1*c*19···C10 (**5**), C12···N2 (**6**), C13···C10 (**7**), C9···C10 (**8**) and C9···C2 (**9**) for the cation of **I**, O2–H2*o*2···N3 (**1**), O2–H1*o*2···N2 (**2**), N4–H1*n*4···N6 (**3**), C15–H1*c*15···N1 (**4**), C11–H1*c*11···N6 (**5**), C8–H1*c*8···C4 (**6**), C8–H1*c*8···C1 (**7**), C13–H1*c*13···C6 (**8**) and C13···N1 (**9**) for the cation of **II**.

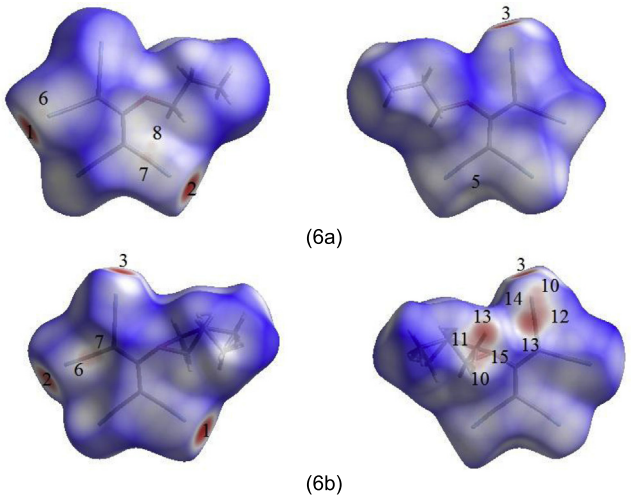

Fig. 6. Views of the Hirshfeld surfaces in two orientations for the $(tcnopr)^-$ anion of **I** & **II**: (HSs are mapped with d_{norm}). The similar labels are as introduced in Fig. 5 and the other labels are as follows: C18–H1*c*18*b*···N6 (**10**), C18–H2*c*18*b*···N6 (**11**), C18–H2*c*18*b*···C7 (**12**), C18···H2*c*18*b*···C1 (**13**), C18*b*···C7 (**14**) and C18*b*···N6 (**15**).

gen atoms of the complex and nitrogen atoms of the $(tcnopr)^-$ anion. The other large red spot, with label 3 in the same figures, is in accordance with N–H···N hydrogen bond which occurs between the cationic unit and the $(tcnopr)^-$ anion.

Several small and pale red spots in the related HSs of **I** and **II** are observed, which are in agreement with existence of weak C–H···N interactions. In these interactions some of the carbon atoms of pyridyl rings act as donors and some of the nitrogen atoms of anions act as acceptors (Fig. 5a: label 4, Fig. 5b: labels 4 & 5, Fig. 6b, labels 10 and 11). There are also some significant C–H···C interactions in the HSs of **I** and **II** which are appeared as small and bright red areas in Figs. 5a and 6a (label 5), Fig. 5b (labels 6–8) and Fig. 6b (labels 6, 7, 12 and 13). The next remaining bright areas are consistent with short C···C and C···N contacts in **I** and **II** (Figs. 5a and 6a: labels 6–9, Fig. 5b: label 9, Fig. 6b: labels 14 and 15).

The red spots with labels 10–15 in HSs of compound **II** are due to the interaction of two $(tcnopr)^-$ anions, *via* chain **b** of CH_3CH_2-CH_2 disordered group in one anion and via the nitrile part in another anion (as noted in the X-ray section). These interactions only occur in structure **II**. These contacts will not be further discussed as they do not represent a real contact in the crystal structure and the configurations forming disorder do not occur in the same unit cell.

As discussed above in the X-ray description section, in both structures, there are anion···π interactions between some of the nitrogen atoms of $(tcnopr)^-$ anion and aromatic pyridyl rings of coordinated ligands, and these interactions can be considered weak. The HS mapped with the shape-index function does illustrate the anion···π interactions quite conclusively. This map has been typically given for structure **I**, in Fig. 7, which includes more anion...π interactions with regard to those in structure **II**.

Finally, in order to obtain more information of the crystal packing, the two-dimensional FPs for each component of **I** and **II** were analyzed (Figs. S3–S6). The full fingerprint plots of the Zn complex cation and the related counter anion are shown in Figs. S3a and S4a. For the Cd compound, two input files were constructed (**II**a and **II**b) and the full FPs of cations and anions in **II**a and **II**b are shown in Figs. S5a, S5e (cations), S6a and S6e (anions).

The full plots were also divided to the partial interactions in order to analysis of major forces contributing to the cohesion of components in the crystal structures of **I** and **II**.

The decomposed fingerprint plots show that the percentages of interactions in the components of **I** and **II** are very close to each other. Survey of these plots for cation components demonstrated the H···H van der Waals forces represent the major contribution portion received by the cations (37.3% in **I**, Fig. S3b, 35.9% in **II**a, Fig. S5b and 37.9% in **II**b, Fig. S5f).

For the $(tcnopr)^-$ anions, N···H/H···N interactions (39.0% in **I** and 41.6% in **II**a and 43.2% in **II**b) have the highest contributions to the total anion HSs and appear as distinct and short spikes in the related FPs (see Figs. S4b, S6b and S6f).

The H···N fingerprint plots in $M[O]_2[N]_2$ cations have more concentration of points in the upper part of diagonal in the plot, which is caused by the fact that nitrogen acceptors of H bonds are situated outside of the surface. The shortest contacts (*i.e.*, $d_e + d_i$) near the 2.0 Å in the H···N fingerprint plots of both structures correspond to the aqua H-atoms interacting with N atoms of anionic moieties (Figs. S3c, S5c and S5g). These interactions are responsible for the formation of 3D networks of the structures **I** and **II**.

The C···H/H···C short contacts are the other important interactions in **I** and **II** with almost equal contribution portions to the crystals, which are represented by two short spikes in the corresponding FPs (Figs. S3d–S6d, S5h and S6h). In addition to the aforementioned interactions, some other close contacts such as C···C, C···N and O···H exist in the crystal structures **I** and **II**, that have quite small participation portions in the total Hirshfeld surfaces.

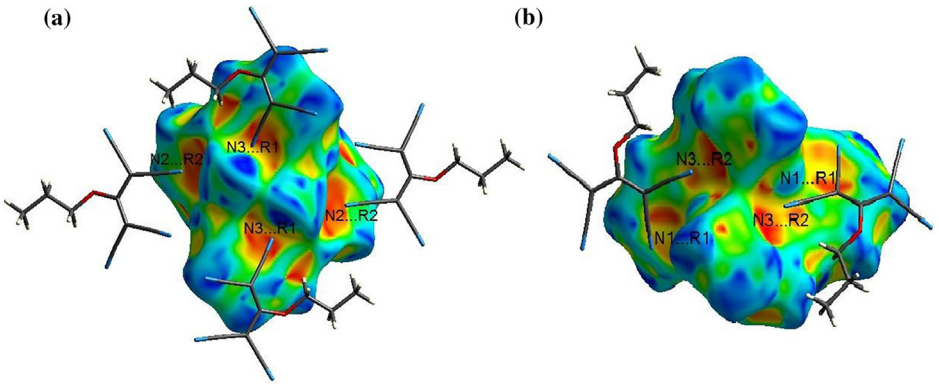

Fig. 7. Hirshfeld surface of $Zn[O]_2[N_2]_2$ cation of **I** mapped with the shape-index function, showing the presence of anion–π interactions. Interacting anions are shown as a tube model in 2 orientations (a and b).

4. Concluding remarks

The results presented above have shown that the Zn and Cd compounds show common octahedrally-based cationic structure, surrounded by not-coordinated anions. The major intermolecular interactions are hydrogen bonds, where the CN groups of the anion accept H bonds from the coordinated water hydrogens (4×) and from the N–H group of the dipyridylamine (2×). In this way 6 of the 8 nitrile groups in the two tcnopr$^-$ anions accept a hydrogen bond. Interesting anion-π interactions, between the aromatic rings of the cation and the nitrile groups of the non-coordinating tcnopr$^-$ anion are observed, in which three CN groups are involved. The non-H-bond acceptor nitrile is also not involved in the anion-π interactions. The Hirshfeld surface analysis was used to visualize moderate and weak hydrogen bonds and anion···π-stacking in the structures. The slightly differences in the packing maps of the structures were discussed based on the different contribution portions of various contacts in the crystals. The difference in packing mostly consists in the weaker interactions, typically anion···π, which revealed as four and three symmetry-independent interactions for Zn and Cd compounds, respectively.

Both compounds show a moderate to weak luminescence in the solid state at room temperature.

Acknowledgements

The authors are indebted to the Algerian DGRSDT (Direction Générale de la Recherche Scientifique et du Développement Technologique) for financial support.

The crystallographic part was supported by the project 15-12719S of the Czech Science Foundation using instruments of the ASTRA lab established within the Operation program Prague Competitiveness – project CZ.2.16/3.1.00/24510.

Appendix A. Supplementary data

CCDC 1517309 (Cd compound) and 1517311 (Zn compound) contains the supplementary crystallographic data. These data can be obtained free of charge via http://dx.doi.org/10.1016/j.poly.2017.04.020, or from the Cambridge Crystallographic Data Centre, 12 Union Road, Cambridge CB2 1EZ, UK; fax: (+44) 1223-336-033; or e-mail: deposit@ccdc.cam.ac.uk. Supplementary data associated with this article can be found, in the online version, at http://dx.doi.org/10.1016/j.poly.2017.04.020.

References

[1] P. Pust, V. Weiler, C. Hecht, A. Tucks, A.S. Wochnik, A.K. Henss, D. Wiechert, C. Scheu, P.J. Schmidt, W. Schnick, Nat. Mater. 13 (2014) 891.
[2] C.F. Zhu, S. Chaussedent, S.J. Liu, Y.F. Zhang, A. Monteil, N. Gaumer, Y.Z. Yue, J. Alloy. Compd. 555 (2013) 232.
[3] X. Liu, A. Gonzalez-Castro, I. Mutikainen, A. Pevec, S.J. Teat, P. Gamez, J.S. Costa, E. Bouwman, J. Reedijk, Polyhedron 110 (2016) 100.
[4] X. Liu, E. Bouwman, Polyhedron 118 (2016) 25.
[5] H. Kim, G.R. You, G.J. Park, J.Y. Choi, I. Noh, Y. Kim, S.J. Kim, C. Kim, R.G. Harrison, Dyes Pigment. 113 (2015) 723.
[6] X. Liu, S. Akerboom, M. de Jong, I. Mutikainen, S. Tanase, A. Meijerink, E. Bouwman, Inorg. Chem. 54 (2015) 11323.
[7] X.H. Qian, Z.C. Xu, Chem. Soc. Rev. 44 (2015) 4487.
[8] M. de Torres, S. Semin, I. Razdolski, J.L. Xu, J. Elemans, T. Rasing, A.E. Rowan, R.J. M. Nolte, Chem. Commun. 51 (2015) 2855.
[9] F.A. Mautner, F.R. Louka, J. Hofer, M. Spell, A. Lefevre, A.E. Guilbeau, S.S. Massoud, Cryst. Growth Des. 13 (2013) 4518.
[10] F.A. Mautner, M. Scherzer, C. Berger, R.C. Fischer, S.S. Massoud, Inorg. Chim. Acta 425 (2015) 46.
[11] F.A. Mautner, M. Scherzer, C. Berger, R.C. Fischer, R. Vicente, S.S. Massoud, Polyhedron 85 (2015) 20.
[12] P. Gamez, T.J. Mooibroek, S.J. Teat, J. Reedijk, Accounts Chem. Res. 40 (2007) 435.
[13] Z.L. Lu, P. Gamez, I. Mutikainen, U. Turpeinen, J. Reedijk, Cryst. Growth Des. 7 (2007) 1669.
[14] T.J. Mooibroek, P. Gamez, Inorg. Chim. Acta 360 (2007) 381.
[15] S.R. Choudhury, B. Dey, S. Das, P. Gamez, A. Robertazzi, K.T. Chan, H.M. Lee, S. Mukhopadhyay, J. Phys. Chem. A 113 (2009) 1623.
[16] P. de Hoog, A. Robertazzi, I. Mutikainen, U. Turpeinen, P. Gamez, J. Reedijk, Eur. J. Inorg. Chem. (2009) 2684.
[17] A. Das, S.R. Choudhury, B. Dey, S.K. Yalamanchili, M. Helliwell, P. Gamez, S. Mukhopadhyay, C. Estarellas, A. Frontera, J. Phys. Chem. B 114 (2010) 4998.
[18] A. Frontera, P. Gamez, M. Mascal, T.J. Mooibroek, J. Reedijk, Angew. Chem., Int. Ed. 50 (2011) 9564.
[19] T.J. Mooibroek, P. Gamez, J. Reedijk, CrystEngComm 10 (2008) 1501.
[20] A. Addala, F. Setifi, K.G. Kottrup, C. Glidewell, Z. Setifi, G. Smith, J. Reedijk, Polyhedron 87 (2015) 307.
[21] C. Atmani, F. Setifi, S. Benmansour, S. Triki, M. Marchivie, J.Y. Salaun, C.J. Gomez-Garcia, Inorg. Chem. Commun. 11 (2008) 921.
[22] S. Benmansour, C. Atmani, F. Setifi, S. Triki, M. Marchivie, C.J. Gomez-Garcia, Coord. Chem. Rev. 254 (2010) 1468.
[23] S. Benmansour, F. Setifi, C.J. Gomez-Garcia, S. Triki, E. Coronado, J.Y. Salaun, J. Mol. Struct. 890 (2008) 255.
[24] S. Benmansour, F. Setifi, S. Triki, J.Y. Salaun, F. Vandevelde, J. Sala-Pala, C.J. Gomez-Garcia, T. Roisnel, Eur. J. Inorg. Chem. (2007) 186.
[25] Z. Setifi, F. Setifi, L. El Ammari, M. El-Ghozzi, J.S.D. Santos, H. Merazig, C. Glidewell, Acta Crystallogr., Sect. C 70 (2014) 19.
[26] B.L. Schottel, H.T. Chifotides, M. Shatruk, A. Chouai, L.M. Perez, J. Bacsa, K.R. Dunbar, J. Am. Chem. Soc. 128 (2006) 5895.
[27] X.P. Zhou, X.J. Zhang, S.H. Lin, D. Li, Cryst. Growth Des. 7 (2007) 485.
[28] S.R. Choudhury, C.Y. Chen, S. Seth, T. Kar, H.M. Lee, E. Colacio, S. Mukhopadhyay, J. Coord. Chem. 62 (2009) 540.
[29] L. Palatinus, G. Chapuis, J. Appl. Crystallogr. 40 (2007) 786.
[30] V. Petricek, M. Dusek, L. Palatinus, Z. Kristall. 229 (2014) 345.
[31] Diamond, Crystal Impact GbR ver 3.1e, Bonn (Germany) 2007.
[32] F. Thetiot, S.F. Triki, J.S. Pala, Polyhedron 22 (2003) 1837.
[33] S. Majumder, L. Mandal, S. Mohanta, Inorg. Chem. 51 (2012) 8739.
[34] Z. Li, A. Dellali, J. Malik, M. Motevalli, R.M. Nix, T. Olukoya, Y. Peng, H.Q. Ye, W. P. Gillin, I. Hernández, P.B. Wyatt, Inorg. Chem. 52 (2013) 1379.
[35] B. Dutta, P. Bag, U. Flörke, K. Nag, Inorg. Chem. 44 (2005) 147.
[36] W. Chen, Q. Peng, Y.D. Li, Cryst. Growth Des. 8 (2008) 564.
[37] S. Banthia, A. Samanta, J. Phys. Chem. B 110 (2006) 6437.
[38] Z. Setifi, K.V. Domasevitch, F. Setifi, P. Mach, S.W. Ng, V. Petricek, M. Dusek, Acta Crystallogr., Sect. C 69 (2013) 1351.
[39] A. Bondi, J. Phys. Chem. 68 (1964) 441.
[40] J.J. McKinnon, D. Jayatilaka, M.A. Spackman, Chem. Commun. (2007) 3814.
[41] S.K. Seth, CrystEngComm 15 (2013) 1772.
[42] M.A. Spackman, J.J. McKinnon, CrystEngComm 4 (2002) 378.
[43] S.K. Wolff, D.J. Grimwood, J.J. McKinnon, M.J. Turner, D. Jayatilaka, M.A. Spackman, University of Western Australia, Perth 2012.